DISCLAIMER

Light Induced Charge Transport within a Single Asymmetric Nanowire

Chong Liu,[†, §, ⊥] *Yun Jeong Hwang,*[†, §, ⊥] *Hoon Eui Jeong,*[†] *Peidong Yang*[*, †, ‡, §]

[†] Department of chemistry, and [‡] Department of Materials Science and Engineering, University of California, Berkeley, California 94720,

[§]Materials Sciences Division, Lawrence Berkeley National Laboratory, Berkeley, California 94720

RECEIVED DATE (to be automatically inserted after your manuscript is accepted if required according to the journal that you are submitting your paper to)

To whom correspondence should be addressed: Email: p_yang@berkeley.edu

⊥ These authors contributed equally to this work

ABSTRACT

Artificial photosynthetic systems using semiconductor materials have been explored for more than three decades in order to store solar energy in chemical fuels such as hydrogen. By mimicking biological photosynthesis with two light-absorbing centers that relay excited electrons in a nanoscopic space, a dual-band gap photoelectrochemical (PEC) system is expected to have higher theoretical energy conversion efficiency than a single band gap system. This work demonstrates the vectorial charge transport of photo-generated electrons and holes within a single asymmetric Si/TiO_2 nanowire using Kelvin probe force microscopy (KPFM). Under UV illumination, higher surface potential was observed on the n-TiO_2 side, relative to the potential of the p-Si side, as a result of majority carriers' recombination at the Si/TiO_2 interface. These results demonstrate a new approach to investigate charge separation and transport in a PEC system. This asymmetric nanowire heterostructure, with a dual band gap configuration and simultaneously exposed anode and cathode surfaces represents an ideal platform for the development of technologies for the generation of solar fuels, although better photoanode materials remain to be discovered.

KEYWORDS: charge separation, Kelvin Probe Force Microscopy (KPFM), asymmetric nanowire, dual band gap configuration, solar water splitting

MANUSCRIPT TEXT

A semiconductor used for direct solar water splitting[1,2] is required to be photo-electrochemically stable, to have an appropriate band gap that can support broad absorption of the solar spectrum as well as band edges at suitable potentials for the water reduction/oxidation half reactions, and to perform fast charge transfer at the semiconductor/electrolyte interface and efficient evolution of hydrogen and oxygen.[1,3] Because of the stringent requirements on the band gap and band edge energies, early research efforts have focused on semiconductors with relatively large band gaps, which are mostly UV-absorbing semiconductors.[4-6] On the other hand, the dual-band gap approach enables the usage of smaller band gap materials for much better coverage of the solar spectrum,[7] and it was predicted that such a scheme could lead to a PEC system with energy conversion efficiency as high as $\eta = 27\%$.[8]

In natural photosynthetic systems,[9] a process involving two photons is in operation for the oxidation of water and storage of the solar energy in sugar. Similarly, in an ideal dual-band gap PEC cell,[7] two photons could be used to excite the two semiconductors that are in close contact. The minority carriers of the two semiconductors will oxidize and reduce water, while the majority carriers recombine at the semiconductor junction. Chemical redox mediators or metal can be introduced for fast electron transfer between the two semiconductors.[10,11] In this work, an asymmetric Si/TiO_2 core/shell nanowire heterostructure was designed (Figure 1a) to explore the feasibility of such a dual-band gap scheme for direct solar water splitting. Although TiO_2 has been widely studied in photo-degradation for environmental applications and water splitting, its wide band gap, fast carrier recombination and back reaction limit the energy conversion efficiency[12-14]. Silicon, on the other hand, possesses the proper conduction band edge for reduction of water to generate H_2 and absorbs visible light [15-17]. These asymmetric Si/TiO_2 nanowire heterostructures are desirable for direct solar water splitting with the water oxidation reaction on the TiO_2 surface and the reduction reaction on the Si surface. In this study, charge separation within this asymmetric structure is observed at the single nanowire level. Using KPFM[18]under conditions that mimic the environment of real water splitting, the light-induced local surface potential change within a single asymmetric nanowire is mapped to demonstrate the proposed spatial charge separation mechanism,. These experiments suggest that a dual-band gap asymmetric configuration with exposed anode and cathode surfaces induce charge separation at semiconducotor/electrolyte interface. Such a structure represents an ideal platform for the development of technologies to generate solar fuels.

The asymmetric Si/TiO_2 core-shell nanowire structures were synthesized with one part consisting of a Si nanowire and the other part consisting of a Si/TiO_2 core-shell structure (Figure 1a). This asymmetric structure ensures large contact area and charge separation/collection efficiency across the semiconductor/semiconductor and the semiconductor/electrolyte junction.[15,19-21] A detailed synthesis scheme is illustrated in Supplementary Figure S1. Si nanowires were grown vertically on a Si (111) substrate via the vapor-liquid-solid (VLS) mechanism,[22] and the amorphous TiO_2 shell was conformally coated by atomic layer deposition (ALD) at 80 ^oC. With the bottom half of the structures protected by photoresist, the top part of the TiO_2 shell was removed by HF etchant, which resulted in arrays of asymmetric Si/TiO_2 core/shell nanowires (Fig 1b). Additional annealing at 600 ^oC transformed amorphous TiO_2 into the anatase structure, which was confirmed by X-ray diffraction (XRD) and transmission electron microscopy (TEM).

Scanning electron microscopy (SEM) and TEM images show that these asymmetric Si/TiO_2 nanowires are typically 5~6 μm in length, with a Si core of 120 nm in diameter and a TiO_2 layer of 30 nm in thickness (Fig. 1c-f). A sharp junction between the Si and Si/TiO_2 core/shell parts was generated, and the nanowires remained vertical on the Si substrate after all the processing steps. The TiO_2 layer often had single-crystalline domains of up to 100 nm.[19]

For such asymmetric nanowire heterostructures with the dual-band gap configuration, electron-hole pairs can be generated in the silicon and TiO_2 using photons of different wavelengths. Because of the band-bending of the space-charge layer at the semiconductor/electrolyte interface,[3] solar illumination would leave positively charged holes on the n-TiO_2 side (anode behavior) and negatively charged electrons on the p-Si side (cathode behavior), with the recombination of majority carriers between the two semiconductors (Figure 2a). As the result, a dipole along the asymmetric nanowire is expected with more positive electrical potential in the n-TiO_2 part relative to that of the p-Si part when both the Si and TiO_2 absorb light (Figure 2a-b). The minority carriers of both semiconductors, with proper energetics, are ready to perform a complete water splitting reaction.[7]

To examine this charge separation, KPFM[18] was used to map the surface potential distribution of an isolated asymmetric nanowire (Figure 2c-f). An asymmetric Si/TiO_2 nanowire was transferred onto an insulating fused silica substrate and 365 nm UV light was applied to excite both Si and TiO_2[23] (Supplementary Figure S2). Controlled humidity was applied to condense water onto the nanowire surface[24-26] and to establish semiconductor/electrolyte interfaces. In the dark, the surface potential of the Si/TiO_2 core/shell part is about 15 mV higher than that of the Si-only part (Figure 2d), mainly due to the work function difference between these two materials[18]. Under UV illumination, the local surface potential of the Si/TiO_2 part is significantly more positive (by 60 mV) than that of the Si (Figure 2e), indicating positive charge buildup on the Si/TiO_2 part as expected. This photoresponse of the surface potential is reversible (Figure 2f), suggesting that the change of the surface potentials originates from UV illumination. Control experiments with both pristine Si nanowires and complete Si/TiO_2 core/shell nanowires showed no comparable surface potential changes (See Supplementary Figure S3 and Figure

S4). Changing the wavelength of illumination to 465 nm also gave no significant change in the surface potential's profile (See Supplementary Figure S5). Photo-excitation of both semiconductors, and in this case UV-activation of TiO_2, was necessary for effective charge separation and dipole formation.

The surface potential difference between the Si and Si/TiO_2 increased gradually as the light intensity was increased (Figure 3). The surface potentials on the Si/TiO_2 part were not uniform under illumination (Figure 3a), probably because of the domain structure of the TiO_2 shell. Despite this non-uniform profile, the trend of saturation at high light intensity (Figure 3b) is in accordance with the expected behavior of the dual-band gap configuration, with flatting of the band at the semiconductor/electrolyte interface.[7,8] The result also suggests that photo-generated minority holes in the TiO_2 layer and electrons in the Si core can be efficiently separated in our asymmetric core/shell nanostructures.

As a powerful technique to resolve the surface potential of materials spatially, KPFM has been widely applied in surface chemistry, light emitting diodes, and solar cells.[18,23,27] In this study, we applied this technique to a photoelectrochemically relevant nanostructure, and examined the photo-responses of the surface potential at the semiconductor/electrolyte and semiconductor/semiconductor heterojunctions. The light-induced charge transport within an asymmetric nanowire was observed through KPFM in a dual-band gap configuration, indicating that the minority carriers of the semiconductors are separated while the majority carriers of the semiconductors recombine at the interface. This asymmetric nanostructure design using the dual-band gap configuration is applicable to other semiconductors, and the overall solar energy conversion efficiency can potentially be improved by coupling two visible light absorbers which balance the photo-excited carrier generation rate upon solar irradiation.[7,8]

ACKNOWLEDGMENT

We thank S. Brittman and A. Zhao for helpful discussions. This work was supported by the Director, Office of Science, Office of Basic Energy Sciences, Materials Sciences and Engineering Division, of the U.S. Department of Energy under Contract No. DE-AC02-05CH11231.

SUPPORTING INFORMATION

Synthesis details of the asymmetric nanowires and control experiments of the KPFM measurement. This material is available free of charge via the Internet at http://pubs.acs.org.

FIGURE CAPTIONS

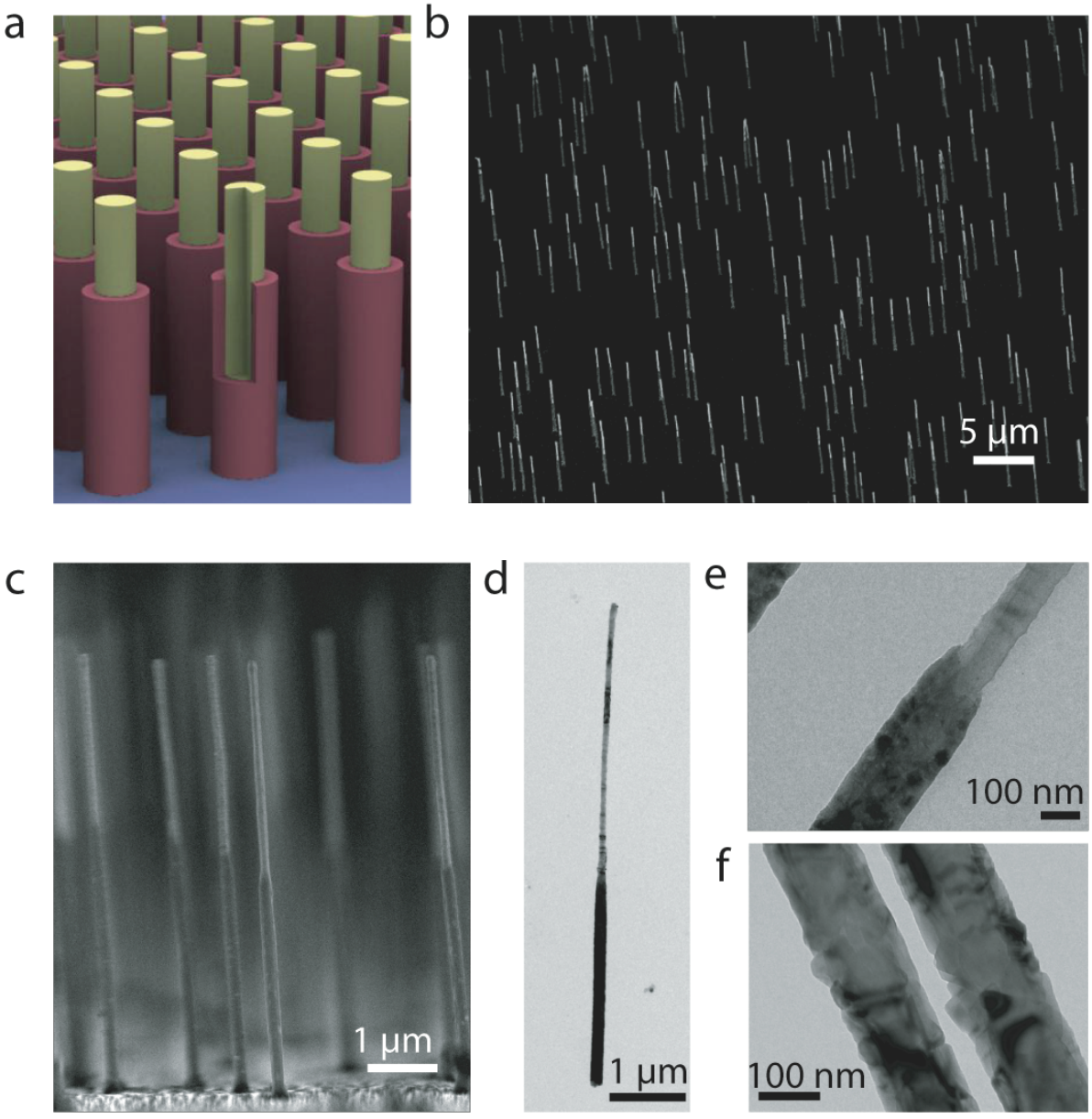

Figure 1. **a**, Schematic illustration of the asymmetric nanowires, with silicon core (yellow) and TiO_2 shell (red). **b**, Corresponding tilted SEM image of the asymmetric nanowires grown vertically on a Si(111) substrate, and **c**, a cross-sectional SEM image of the asymmetric nanowires, showing the contrast difference between the top Si (bright) and the bottom Si/TiO_2 (dark) parts. **d-f**, TEM images of asymmetric nanowires, indicating the sharp Si/TiO_2 junctions (**e**), and core-shell TiO_2/Si structure (**f**).

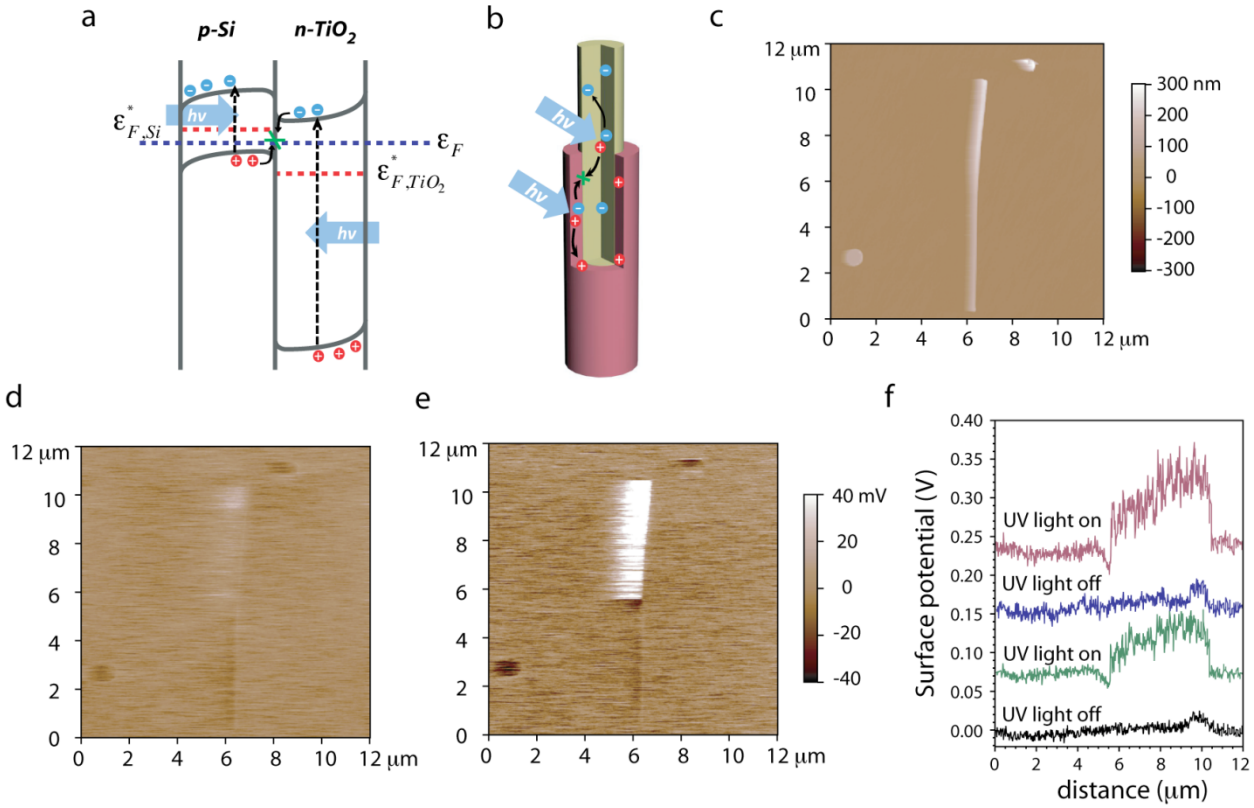

Figure 2. a, Schematic energy diagram of charge separation for the Si/TiO_2 dual-band gap configuration. The Fermi level in dark (dashed blue) and quasi-Fermi levels under illumination (dashed red) are shown. For simplicity, a uniform distribution of quasi-Fermi level is assumed within each part of the asymmetric nanowire. **b**, Schematic of the spatial charge distribution within an asymmetric nanowire under illumination according to (**a**). **c**, Topographical AFM image of the asymmetric nanowire and measured surface potential mapping of an asymmetric nanowire in the dark (**d**) and under 365 nm UV illumination with 4.5 mW/cm^2 intensity (**e**). **f**, Surface potential profiles along an asymmetric nanowire from Si (distance 0 µm) to Si/TiO_2 measured under the same light intensity as in **e**. The curves are offset for clarity. The data were collected sequentially from bottom to top, switching between dark and UV illumination.

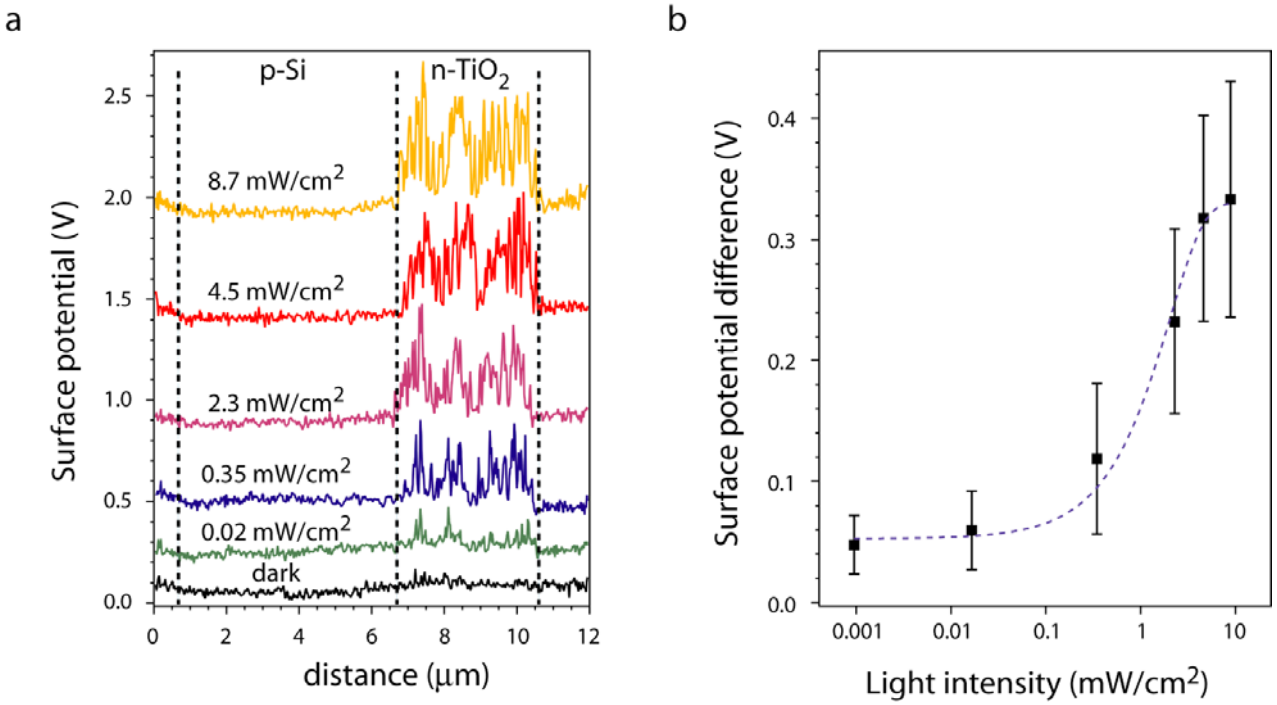

Figure 3. a, Surface potential profile of an asymmetric nanowire measured at different light intensities. The potential profiles are offset for clarity. **b**, Averaged surface potential difference between the Si/TiO_2 core-shell region and the Si region, and its dependence on the intensity of the 365 nm UV light. The error bars on the data indicate the spatial variation of the surface potential of the Si/TiO_2 core-shell region as compared to the averaged value of the Si region caused by the heterogenity of the photoresponse among TiO_2 domains. The average was calculated from multiple samples with different scan parameters performed at the same light intensity.

REFERENCES

(1) Walter, M. G.; Warren, E. L.; McKone, J. R., Boettcher, S. W.; Mi, Q.; Santori, E. A.; Lewis, N. S.; *Chem. Rev*., **2010**, *110*, 6446-6473

(2) Fujishima, A.; Hongda, K.; *Nature*, **1972**, *238*, 37-38

(3) Grätzel, M.; *Nature*, **2001**, *414*, 338-344

(4) (a) Khan, S. U. M.; Al-Shahry, M.; Ingler Jr., W. B.; *Science*, **2002**, *297*, 2243-2245 (b) Chem., X.; Liu, L.; Yu, P. Y.;

Mao, S. S.; *Science*, **2011**, *331*, 746-750

(5) Tiley, S. D.; Cornuz, M.; Sivula, K.;, Grätezl, M.; *Agnew. Chem. Int. Ed*., **2010**, *49*, 6405-6408

(6) Lu, D.; Takata, T.; Saito, N.; Inoue, Y.; Domen, K.; *Nature*, **2006**, *440*, 295

(7) Nozik, A. J., *Appl. Phys. Lett*., **1976**, *29*, 150-153

(8) Bolton, J. R.; Strickler, S. J.; Connolly, J. S.; *Nature*, **1985**, *316*, 495-500

(9) Raven, P. H.; Evert, R. F.; Eichhorn, S. E., *Biology of Plants*, *7th Ed.,* 124-127 (W. H. Freeman and Company Publishers, New York, 2005)

(10) Hiroaki, T.; Mitsui, T.; Kiyonaga, T.; Akita, T.; Tanak, K.; *Nature Mater*., **2006**, *5*, 782-786

(11) Abe, R.; Sayama, K.; Sugihara, H.; *J. Phys. Chem. B*, **2005**, *109*, 16052-16061

(12) Serpone, N.; Lawless, D.; Khairutdinov, R.; *J. Phys. Chem*., **1995**, *99*, 16655-16661

(13) Bahnemann, D. W.; Hilgendorff, M.; Memming, R.; *J. Phys. Chem. B*, **1997**, *101*, 4265-4275

(14) Cowan, A. J.; Tang, J.; Leng, W.; Durrant, J. R.; Klug, D. R.; *J. Phys. Chem. C*, **2010**, *114*, 4208-4214

(15) Boettcher, S. W.; Spurgeon J.; Putnam, M. C.; Warren, E. L.; Turner-Evans, D. B.; Kelzenberg, M. D.; Maiolo, J. R.; Atwater, H. A.; Lewis, N. S.; *Science*, **2010,** *327*, 185-187

(16) Boettcher, S. W.; Warren, E. L.; Putnam, M. C.; Santori, E. A.; Turner-Evans, D.; Kelzenberg, M. D.; Walter, M. G.; McKone, J. R.; Brunschwig, B. S.; Atwater, H. A.; Lewis, N. S.; *J. Am. Chem. Soc*., **2011**, *133*, 1216-1219

(17) Hou, Y.; *et al*.; *Nature Mater*., **2011**, ASAP

(18) Liscio, A.; Palermo, V.; Samori, P.; *Acc. Chem. Res*., **2010**, *43*, 541-550

(19) Hwang, Y. J.; Boukai, A.; Yang, P.; *Nano Lett*., **2009**, *9*, 410-415

(20) Law, M.; Greene, L. E.; Johnson, J. C.; Saykally, R.; Yang, P.; *Nature Mater*., **2005**, *4*, 455-459

(21) Tian, B.; Zheng, X.; Kempa, T. J.; Fang, Y.; Yu, N.; Yu, G.; Huang, J.; Lieber, C. M.; *Nature*, **2007**, *449*, 885-889

(22) Hochbaum, A. I.; Fan, R.; He, R.; Yang, P.; *Nano Lett*., **2005**, *5*, 457-460

(23) Coffey, D. C.; Ginger, D. S.; *Nature Mater*., **2006**, *5*, 735-740

(24) Fan, F. F.; Bard, A. J.; *Science*, **1995**, *270*, 1849-1852

(25) Verdaguer, A.; Weis, C.; Oncins, G.; Ketteler, G.; Bluhm, H.; Salmeron, M.; *Langmuir*, **2007**, *23*, 9699-9703

(26) Salmeron, M.; Bluhm, H.; Tatarkhanov, M.; Ketteler, G.; Shimizu, T. K.; Mugarza, A.; Deng, X.; Herranz, T.; Yamamoto, S.; Nilsson, *A.; Faraday Discuss.*, **2009**, *141*, 221-229

(27) Slinker, J. D.; DeFranco, J. A.; Jaquith, M. J.; Silveira, W. R.; Zhong, Y.; Moran-Mirabal, J. M.; Cralghead, H. G.; Abruna, H. D.; Marohn, J. A.; Malliaras, G. G.; *Nature Mater*., **2007**, *6*, 894-899

TOC

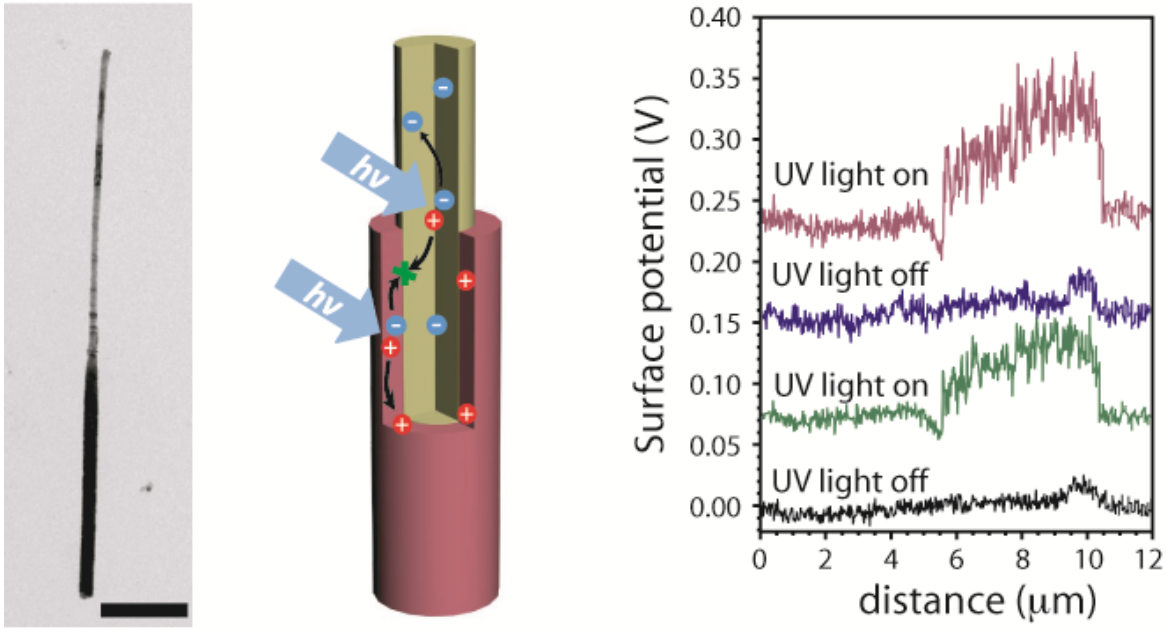

Acknowledgements: This work was supported by the Director, Office of Science, Office of Basic Energy Sciences, Material Sciences and Engineering Division, of the U.S. Department of Energy under Contract No. DE-AC02-05CH11231. We thank the National Center for Electron Microscopy for the use of their facilities.